AIAA 99-2448

Experiments on Weakly-Ionized Air and Nitrogen Plasmas for Hypersonic Propulsion Facility Development

F.K. Lu, D.R. Wilson
The University of Texas at Arlington
Arlington, TX

H.-C. Liu
National Cheng Kung University
Tainan, TAIWAN

and

W.S. Stuessy
The University of Texas at Arlington
Arlington, TX

35th AIAA/ASME/SAE/ASEE Joint Propulsion Conference and Exhibit
20–24 June 1999
Los Angeles, California

Experiments on weakly-ionized air and nitrogen plasmas for hypersonic propulsion facility development

Frank K. Lu[*] Donald R. Wilson[†] Hsuan-Cheng Liu[‡] and W. Scott Stuessy[§]
University of Texas at Arlington, Arlington, Texas 76019

An experimental investigation of the effect of applied electrical field, static temperature, static pressure and seed concentration on the electrical conductivity of air and nitrogen plasmas under high-enthalpy conditions was performed using a detonation-driven shock tube and a conductivity measurement channel. A pulse of plasma of about 0.5 ms duration flowed past the channel. The conductivity peaked toward the middle of the pulse and decayed toward the contact surface that arrived shortly thereafter. The measurements are compared against values obtained using the Chemical Equilibrium Code. Plasma pressures were 10 and 20 atm while temperatures ranged from 1800 to 3600 K. The observed rise of conductivity with temperature for the seeded air plasma is flatter than theoretical results. Also the observed values of conductivity are considerably lower than theoretical values. At 10 atm, the measured conductivities are lower than theoretical values by a factor of 5 to 13. However, the measured peak conductivities at 20 atm tests are considerably higher than theoretical values. The higher observed conductivities at 20 atm suggests that joule heating may be important. Alternatively, this may be due to non-equilibrium of the plasma. Similar results were found in nitrogen plasmas.

Nomenclature

e	=	electronic charge
I	=	total input current
k	=	Boltzmann constant
M	=	Mach number
MHD	=	magnetohydrodynamic
p	=	pressure
S	=	mass fraction of potassium
t	=	time
T	=	temperature
u	=	speed
V	=	voltage drop along conductivity channel
V_A	=	applied voltage
x	=	axial distance
σ	=	electrical conductivity
$\sigma*$	=	average electrical conductivity

Subscripts

s	=	shock
2	=	post-shock conditions

*Professor and Director, Aerodynamics Research Center, Mechanical and Aerospace Engineering Department. Associate Fellow AIAA.

†Professor and Chairman, Mechanical and Aerospace Engineering Department. Associate Fellow AIAA.

‡Graduate Research Associate, Aerodynamics Research Center, Mechanical and Aerospace Engineering Department; presently, Institute of Aeronautics and Astronautics, National Cheng Kung University, Tainan, Taiwan. Student Member AIAA.

§Faculty Research Associate, Aerodynamics Research Center, Mechanical and Aerospace Engineering Department. Senior Member AIAA.

Introduction

THERE is recent interest in exploiting weakly ionized gas flows for aerodynamic applications. Examples of potential applications include MHD accelerators for hypervelocity facilities,[1,2] MHD generators for power extraction,[3-5] and hypersonic flow control.[6] These applications require improved understanding of the conductivity of high-pressure, high-speed plasmas, a topic which is not well studied in the past. A critical requirement for all of these applications is that the plasma must be sufficiently conductive. Therefore, an understanding of the flow properties such as electrical conductivity, electron density and current discharge characteristics is needed in order to develop the aforementioned technologies.

Specifically, an approach for achieving high enthalpy in aerodynamic facilities is to ionize air by using a small amount of alkali salt.[2] Such a facility utilizes an MHD channel to accelerate the weakly ionized air to hypervelocity conditions in order to provide true simulation of inlet conditions.[7] The use of an MHD accelerator is expected to minimize nonequilibrium effects in the flow. The success of this facility concept hinges critically on understanding the electrical behavior of high-pressure aerodynamic plasmas. While previous experimental studies were limited to pressures of about 0.5 atm,[8,9] the present need is for data at higher pressures. Experimental data are needed to validate theoretical models for calculating the electrical conductivity of seeded plasmas at high-pressure levels. The data would also help in understanding the electrical breakdown characteristics of high-pressure plasmas subjected to intense electric fields.

To support the hypervelocity facility development, an experimental program was initiated to obtain an understanding of high-pressure plasma flows. The objective of this program was to determine the conductivity of
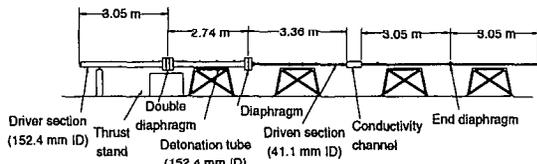
Figure 1: Schematic of detonation-driven shock tube.

lightly-seeded air and nitrogen plasmas at different enthalpy conditions. The data were compared with existing theoretical models.

Experiment

Facility

An existing shock tunnel, upgraded with a detonation driver,[10] and operated as a high-performance shock tube was used to generate the test flow. The converted facility is shown schematically in Fig. 1, while a performance map of the detonation-driven shock tube is shown in Fig. 2. The maximum pressure and temperature achieved are 34 atm and 4200 K, realizing true hypervelocity stagnation conditions. The facility and experimental techniques are briefly described here, and more details can be found in Refs. 5 and 10.

The driver section had a bore of 152.4 mm (6 in.) and a length of 3 m (10 ft). The detonation section also had a bore of 152.4 mm (6 in.) but was 8.23 m (27 ft) long. Both tube sections were rated for a pressure of 41.3 MPa (6000 psi). These two tubes were separated by a double-diaphragm section. The diaphragms were made from 10 or 12 gauge (3.42 or 2.66 mm) steel plates. The detonation and driven sections were separated by a thin mylar diaphragm. The detonation section could
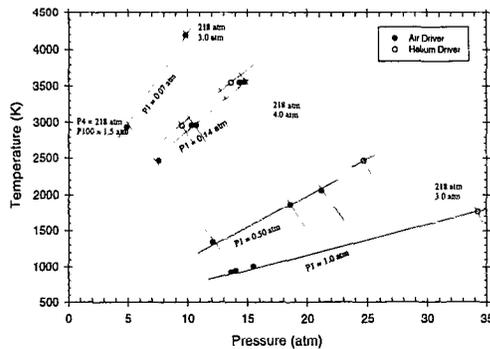

Figure 2: Performance map.

be filled with hydrogen, oxygen and helium. Hydrogen and oxygen were injected through separate tubes for safety purposes. Helium and purge air were injected through the oxygen line. Air, initially in the detonation section, was evacuated through the hydrogen line. After a successful or aborted run, the detonation products were vented through the hydrogen line. Both lines

contain Matheson Series 6103 flash arrestors for added safety. The behavior of the detonation wave was monitored by four wall-mounted pressure transducers.

The driven tube was made of type 304 stainless steel tubing. It had a bore of 41.2 mm (1.62 in) and it was 9 m (30 ft) long. The tube had a pressure rating of 19 MPa (2800 psi). The detonation-driven shock tube was designed for operation in the non-reflected mode. Thus the driven tube was designed for a lower pressure rating. This combination of driver and driven tube produces a driver-to-driven tube area ratio of 14.7 which provides an additional improvement in performance.[11]

The pneumatic system consisted of a Haskell Model 55696 two-stage gas-driven booster pump capable of charging the driver section to 41.3 MPa (6000 psi). The Haskell pump was connected to an air compressor system, consisting of a Clark CMB-6 5-stage air compressor, a twin-tower desiccant drier, and 14.5 MPa (2100 psi) storage bottles. Alternatively, the Haskell pump could be fed from a manifold of 15.2 MPa (2200 psi) helium bottles. The vacuum system consisted of a Sargent-Welch Model 1376 (300 l/min) pump and a Sargent-Welch Model 1396 (2800 l/min) pump for evacuating the driven tube.

Conductivity Channel and Power Supply

Electrical conductivity was measured in a channel connected to the end of the driven section, following Garrison's design.[8] The conductivity measurement channel consisted of a pair of powered electrodes and 20 probe electrodes separated by insulators. The electrodes were made of oxygen-free copper with an electrical resistivity of 1.69 $\mu\Omega\cdot$cm at 300 K. The electrodes had the same inside diameters as the driven tube, with outside diameters of 139.7 mm (5.5 in.). The powered electrodes were 9.53 mm (0.375 in.) thick and they provided an axial electrical field to the flow by discharging a capacitor bank. The 20 electrodes were 3.18 mm (0.125 in.) thick and were used for measuring the voltage drop along the channel. Insulator rings with the same radial dimensions were made from 1.59 mm (0.0625 in.) thick teflon. The total length of the measurement channel, including the powered electrodes, the probe electrodes and the insulators, was 115.9 mm (4.563 in.). The channel dimensions were used to size the power supply.[12] Lexan tubes of 152.4 mm (6 in.) length were mounted on both ends of the conductivity channel to isolate it electrically from the shock tube. As will be subsequently described, the voltage gradient across the 20 probe electrodes was fairly uniform. Thus, the channel yielded a radially averaged conductivity measurement. A capacitor bank, with inductors arranged in a pulse-forming network, delivered the potential across the plasma. It was designed for a maximum charge voltage of 8 kV.

The conductivity channel was wrapped in two sheets of teflon and the subassembly was placed in an aluminum containment structure. This structure extended beyond the ends of the conductivity channel to encase the lexan rings. The containment structure was built to prevent tensile failure of the teflon insulator rings when subjected to peak internal pressures of 10.4 MPa (1500 psi) during the shock-tube blowdown process. The en-

tire conductivity channel assembly was then clamped at each end by two steel plates, tied together with four high-strength bolts, and anchored to the shock-tube thrust stand with high-strength chains. This reinforcement strengthens the axial tie rods which could not sustain tension during the blowdown process.

Seeding System

Potassium carbonate with a purity of 99.9 percent in dry powder form, with a particle size equivalent to 20 mesh, was used. It was stored in a glass bottle with a desiccant to prevent moisture absorption. Nominal seed fractions were one percent of potassium by weight. An Acculab Model V-1mg scale, with a resolution of 1 mg and maximum capacity of 120 g was used to weigh the desired amount of seed material.

The seed injection system was designed to inject the seed into the driven tube as uniformly as possible upstream of the electrical conductivity channel. A chromatography column 86.28 mm (3.937 in.) long, with a bore of 11.11 mm (0.4375 in.), was used to hold the seed. The pressure rating of the column was 4.14 MPa (600 psi). The column was sealed by two endpieces with O-rings and connected to the driven tube by a plastic tube. The plastic tube had a 1.59 mm (0.0625 in.) bore and a 3.18 mm (0.125 in.) outside diameter. It was rated for 3.47 MPa (500 psi). The column was mounted in an aluminum housing which was vibrated by an eccentrically-mounted rubber wheel driven by a small motor to reduce seed coagulation.

Two solenoid valves controlled air flow through the seed injector column. The maximum air pressure through the column was set at 276 kPa (40 psi). During seed injection, the outlet valve was opened first, enabling the seed to be drawn into the driven tube due to the vacuum. Then the inlet valve was opened for few seconds to allow air to blow the seed material into the driven tube. Bench tests of the system indicated that about 10 s was enough to inject the required amount of seed material into the driven tube. The injection raised the driven tube pressure by less than 6.9 kPa (1 psi).

The seed was injected via a T-shaped nozzle assembly, with a pair of nozzles, one facing upstream and another downstream, aligned with the tube axis. This arrangement was a practical way of achieving uniform seeding. The nozzle was inserted into the tube from a cavity in the side of the driven tube by the applied air pressure. Once the pressure was removed, a spring retracted the nozzle back into the cavity to remove it from the flow during a run. A higher inlet air pressure or a longer injection time resulted in a more uniform distribution of the seed material. However, the need to control the initial pressure in the driven tube placed a limit on both inlet air pressure and seed injection time.

Instrumentation and Data Acquisition

The detonation section was instrumented with four flush-mounted PCB model 111A22 dynamic pressure transducers and a MKS model 127A Baratron pressure transducer. The Baratron transducer has a maximum pressure range of 1.33 MPa (10 000 torr), and

was used to set the mixture ratio when filling the detonation driver. The Baratron transducer was also used to provide an initial pressure reading for setting the PCB transducers. The PCB transducers have a full-scale range of 68.9 MPa (10 000 psi), rise time of 2 μs, and a time constant of 1000 s.

The driven section was instrumented with two PCB model 111A23 transducers which have a full-scale pressure range of 34.5 MPa (5000 psi), rise time of 2 μs, and a time constant of 500 s. These transducers, located upstream of the test section, were used primarily for shock speed determination. Two other PCB transducers were either model 111A23 or 111A24, depending upon the conditions in the driven tube. The model 111A24 transducers have a full-scale range of 6.89 MPa (1000 psi), a response time of 2 μs, and a time constant of 100 s. The four transducers monitored the transient conditions in the driven section during a run. The initial pressure in the driven tube was also measured by a MKS model 127A Baratron pressure transducer. This transducer has a maximum pressure range of 133 kPa (1000 torr). It provided an accurate measurement of the initial driven tube pressure as well as serving to initialize the dynamic PCB transducers.

The pressures were sampled simultaneously at 100 kHz and recorded with 12-bit resolution. In addition to a direct indication of pressures, the readings allowed time-of-flight calculations for obtaining detonation or shock wave propagation speeds. The wave speed provided an important indication of the properties of the detonation wave, primarily that the wave had indeed transitioned to a fully-developed Chapman-Jouguet wave. In addition, the wave speed was needed for calculating the properties of the flow past the conductivity channel.

Current and voltages were acquired by the same data acquisition system. Current was measured using a F. W. Bell IHA-150 high-frequency current sensor which measured the magnetic field generated by the electrical current. This sensor was electrically isolated from the circuit. It has a response time of less than 1 μs, a frequency response from DC to 50 kHz, and a full-scale range of ±150 A. Linearity is 1 percent over the compensated temperature range of 0 to 75 °C with an excitation voltage of ±12 VDC. Voltages were stepped down via a divider circuit to match the voltage range of the data acquisition system.

Data Uncertainty

The uncertainty of some key parameters are displayed in Table 1. The initial pressure p_1 was subject to a high degree of uncertainty because the Baratron pressure transducer had to be isolated prior to firing the tunnel to prevent damage resulting from over-pressurization. Small leaks in the conductivity channel allowed the pressure to rise by an unknown amount between isolation of the transducer and diaphragm rupture. This did not affect the accuracy of the shock speed measurements, but adversely affected the ability to precisely set the pressure ratio to achieve a desired shock speed. The uncertainty in average conductivity was due primarily to the uncertainty in determining the extent of the uniform voltage gradient near the power electrodes.
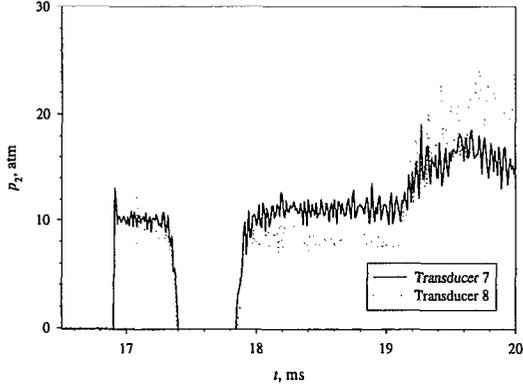
Figure 3: Example of test data: pressure. Transducers 7 and 8 are 75.88 cm and 20.16 cm from the upstream face of the conductivity channel.

Table 1: Data uncertainty.

p_1	±16 %	m_s	±1.3 %
p_2	±5.4 %	S	±1.3 %
T_1	±1.0 %	I	±1.0 %
T_2	±5.5 %	V	±1.0 %
u_2	±1.4 %	$\sigma*$	±4.6 %

Results

Data Analysis

All the runs exhibited similar features and the key features of an example run are now discussed. The nominal conditions for this example are $M_s = 7.76$, $T_2 = 3010$ K, $p_2 = 8.5$ atm, $V_A = 400$ V and $S = 1$ percent. The pressures just upstream of the conductivity channel are shown in Fig. 3. The shock speed u_s was calculated from time-of-flight measurements of shock passage past the two transducers. The shock speed, together with initial conditions, enabled the post-shock pressure p_2 and temperature T_2 to be calculated using TEP, a Microsoft Windows version of the Chemical Equilibrium Code.[16] Previous calibrations indicated agreement between the measured and calculated values for p_2 to within five percent.

It was difficult to ensure repeatability in p_1 because the seals between the electrodes and insulators tended to leak, particularly when p_1 was low. Thus, an inverse calculation using the measured value of p_2 and the measured shock speed was used to obtain p_1. This procedure yielded an accurate determination of test conditions for each run, but precluded good repeatability.

Figure 3 indicated unusual behavior at $t \approx 17.3$ ms during which the measured pressure vanished. This was thought to be due to interference induced in the piezozoresistive pressure transducers from the current flow
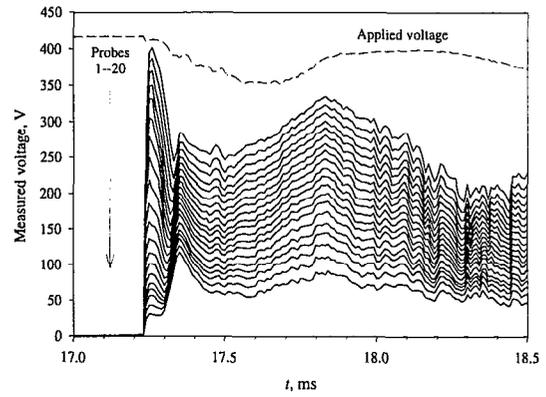

Figure 4: Example of test data: voltage.

in the channel. This phenomenon was not observed at low currents. The abrupt change in transducer output at $t \approx 17.3$ ms coincided with the start of current flow in the channel. The transducer readings returned to a fairly steady level at $t \approx 18.1$ ms. This coincided with the current decaying to near zero.

Figure 4 shows the voltage traces. The top curve is the applied voltage across the powered electrodes. The probe electrodes did not sense any voltage until passage of the ionized flow following the incident shock. The electrode voltages reached a maximum value in about 20 μs and then dropped due to current flowing from the capacitor bank. The estimated test time for this case was about 185 μs. The voltages then rose to a second peak as the applied voltage from the capacitor bank increased.
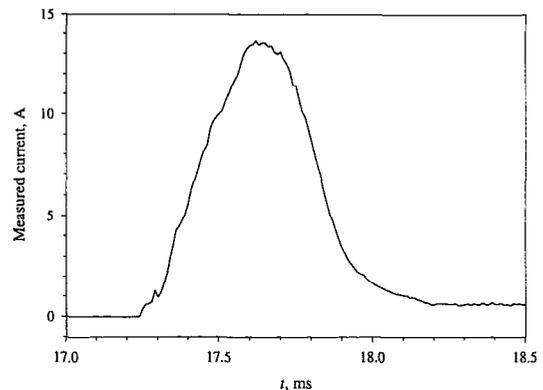

Figure 5: Example of test data: current.

The current peaked at about 17.6 ms, which coincides with the minimum in the applied voltage. This is shown in Fig. 5. The peak current occurred about 210 μs *after* the estimated time for passage of the contact surface through the conductivity channel. The rate of current rise was slower than the designed rate and

4

this was initially thought to be due to an impedance mismatch between the power supply and the plasma load. However, a simulation of the transient characteristics of the power supply by Simmons[21] indicated that the current rise time should be 10–20 μs. The estimated rise times calculated during the design of the power supply were 80–100 μs. Simmons' analysis suggested that a more probable cause of the slow rise time is an actual variation in plasma resistance with time. The plasma resistance variation could be due to the time required for vaporization, dissociation and ionization of the seed. A second possibility would be the non-uniform seed distribution in the driven tube. The residual seed produced measurable conductivity in the detonation products following the test flow, as indicated in the figures.

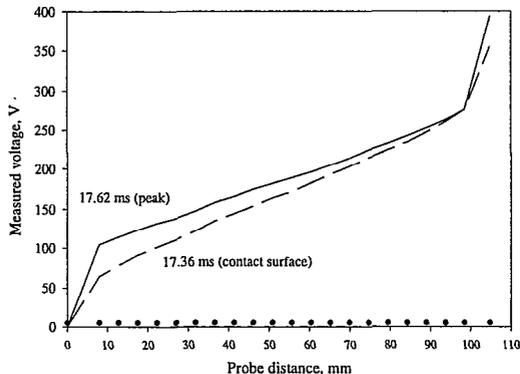Figure 7: Example of test data: voltage difference across the 20 probe electrodes.

Figure 6: Example of test data: voltage gradient. Circles represent midline of the electrodes.

The voltage data were reduced to axial voltage gradients at the time of peak current and at the passage of the contact surface and shown in Fig. 6. The end effects between the power electrodes and the adjacent probe electrodes, in the form of higher voltage gradients, are clearly seen. The voltage across the 20 probe electrodes is shown in Fig. 7. The voltage difference reached a peak of about 250 V and then dropped to about 135 V as the current rose to its peak value at $t \approx 17.6$ ms. This trend was in general agreement with the Nottingham model,[22] which gives the following relation for the electrode voltage drop

$$\Delta V = C_1 + \frac{C_2}{I^n}. \tag{1}$$

The voltage difference then rose, probably due to an increase in boundary layer thickness as the incident shock wave moved downstream.

The average conductivity between the first and last probe electrodes can be expressed as

$$\sigma^*(t) = \frac{I(t)/A}{V_{1-20}(t)/x_{1-20}} \tag{2}$$

where the arguments indicate the transient nature of the flow. The voltage drops between the power electrodes and the adjacent probe electrodes were neglected
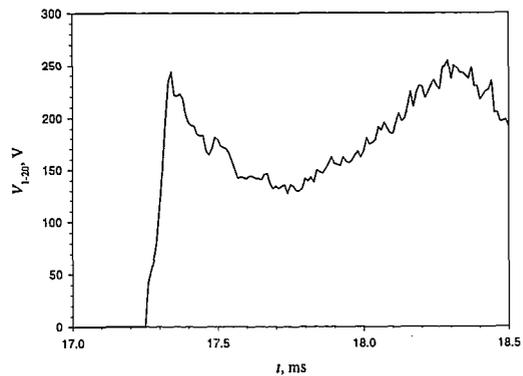
because they included extraneous effects such as surface work functions, voltage drops across the boundary layers, and curvature of current filament lines in the powered electrode region. However, the probe electrodes did not suffer from such effects and the voltage gradient exhibited linear behavior, as can be seen in Fig. 6. The average conductivity, displayed in Fig. 8, closely followed the measured current variation.
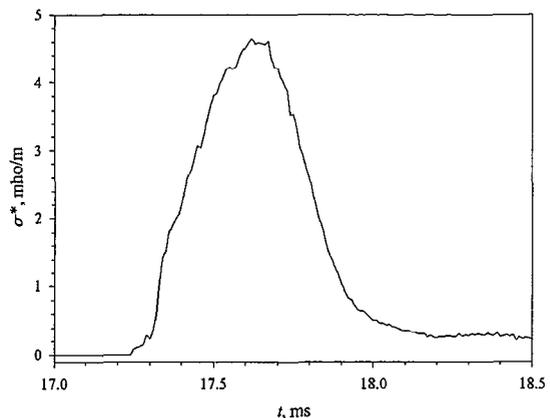

Figure 8: Example of test data: average conductivity.

Comparison with Theoretical Models

Lin et al.[13] have developed a theory for the electrical conductivity of a singly-ionized plasma. A collision mixing model was used to determine the effect of temperature on the electrical conductivity at pressures of about 1 atm. The electrical resistivity can be written as the sum of the resistivity of two effects, namely, those due to electron-neutral and electron-ion collisions, as

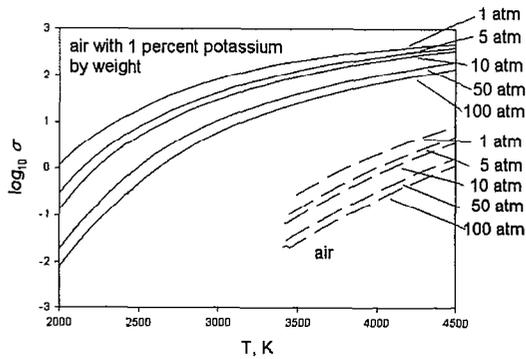$$\frac{1}{\sigma_{add}} = \frac{1}{\sigma_{en}} + \frac{1}{\sigma_{ei}} \tag{3}$$

5

Figure 9: Theoretical conductivity of air with and without potassium seed.

Figure 10: Experimental and theoretical conductivity of air at 10 atm with one percent mass fraction of potassium.

Spitzer and Harm[14] proposed that the electron-ion conductivity could be expressed as

$$\sigma_{ei} = 1.913 \times 10^4 \frac{(kT/e)^{3/2}}{\ln \Lambda} \qquad (4)$$

The quantity kT/e is the gas temperature expressed in electron volts while Λ is a parameter equal to the ratio of Debye shielding distance to the impact parameter for 90-deg scattering by an ion. The conductivity due to electron-neutral collisions σ_{en} can be calculated as a function of the electron density from the Saha equation.[15] However, the conductivity calculated by this method is believed to be overestimated by 70 percent under some circumstances. Thus, more accurate models are definitely needed.

The collision mixing model was used by Garrison[8] to evaluate the conductivity of air for a low pressure, MHD accelerator. He obtained theoretical results for the effect of temperature on electrical conductivity for pressures from 0.1 to 0.5 atm. However, this pressure range is inadequate for facility simulation of airbreathing hypersonic flight. To obtain high-pressure results, the collision mixing model was replaced by a chemical equilibrium model,[16] modified for electrical conductivity calculations by Demetriades and Argyropoulos.[17] Results for pressures from 1 to 100 atm and temperatures from 2000 to 4000 K are shown in Fig. 9 for pure air and for air seeded with one percent by weight of potassium. The figure shows that the theoretical electrical conductivity of seeded air is two to three orders of magnitude higher than pure air. Moreover, the electrical conductivity increases dramatically with temperature but decreases with increased pressure. The theoretical results indicate that there may be difficulties in achieving adequate ionization levels under high-pressure conditions even with seed.

The average conductivity for air at 10 atm is shown in Fig. 10. The data were taken at the peak conductivity and at the arrival of the contact surface at pressures around 10 atm, as indicated in the figure. The figure also shows values at 5, 10 and 15 atm obtained using the above-menti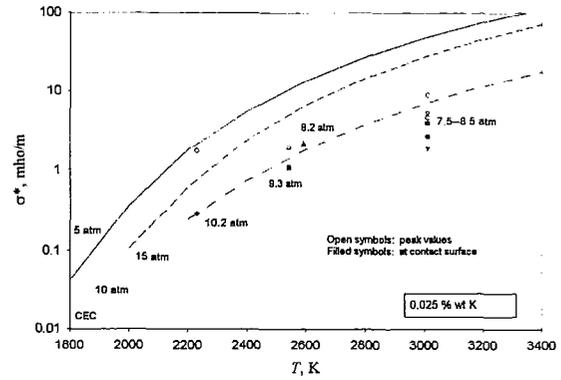oned theory. In general, the measured conductivities were lower than the theoretical values, with the experimental conductivities ranging from 80 percent of theory at low temperatures to 10 percent of theory at the highest temperatures. Figure 10 shows that measured conductivities behind the contact surface were higher than those in front of the contact surface.

Possible reasons for the discrepancy between experiment and theory include boundary layer blockage, joule heating and poor seed entrainment by the flow.[23] The boundary layer blockage reduced the core area for current flow. Accounting for the blockage raised the experimental conductivity, but was not sufficient at the higher temperatures to account for the discrepancy. Joule heating was found to raise the temperature from the front to the rear of the conductivity channel by about 2 K. Its effect on conductivity was, therefore, negligible. Finally, the poor convection of seed appeared to be the most plausible reason for the low experimental values. One indication of this is the presence of current after the slug of test gas has passed. The large particle size resulted in settlement to the bottom of the driven tube between seed injection and run. Moreover, the large particle size also required a long time, of the order of a few ms, for dissociation and ionization to complete. An estimate of the effective seed fraction can be made based on the measured conductivity in air and in the subsequent flow of detonation products. The indication is that only 0.025 percent by weight of potassium was entrained in the test flow, as shown in Fig. 10.

The average conductivity for the nominal 20 atm test runs is presented in Fig. 11. The absolute levels of conductivity are considerably higher than the theoretical predictions for this set of data. Furthermore, a much flatter trend with increased temperature is observed. There is the possibility of leakage current due to a breakdown of the insulators cannot be discounted. (During this sequence of runs, electrical breakdown occurred due to cracks in the teflon rings.)

A comparison between experimental and theoretical conductivities for a seeded nitrogen plasma at 10

6

atm is presented in Fig. 12 for temperatures from 1830 through 3010 K. The flow Mach numbers ranged from 5.49 for the highest temperature through 7.76 for the lowest temperature. Experimental conductivities for seeded nitrogen are higher than for seeded air. The measured conductivity ranged from 75–85 percent of theoretical values at higher temperatures to 2–3 times of theoretical values at lower temperatures. Thus, the phenomenon of electron attachment by positive oxygen ions postulated by Simmons et al.[24] appears to have some degree of validity.

Figure 12: Experimental and theoretical conductivity of nitrogen at 10 atm with one percent mass fraction of potassium.
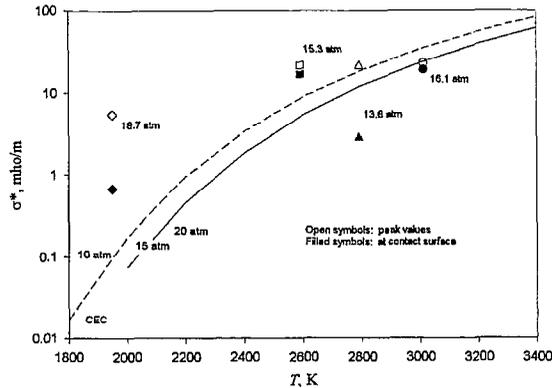
Figure 11: Experimental and theoretical conductivity of air at 20 atm with one percent mass fraction of potassium.

Conclusions

The basic concept first proposed by Garrison[8] was used for measuring electrical conductivity in a shock tube environment. In general, agreement between experimental and theoretical conductivities was fair at nominal pressures of 10 atm for the small amount of seed used. At higher pressures, the experimental conductivities were higher than the theoretical values. However this cannot be validated at present since the possibility of leakage current due to an electrical breakdown within the channel cannot be discounted. Further tests are needed.

The results of the conductivity measurements with a seeded nitrogen plasma appear to give some support to the theory of electron attachment by the positive oxygen ions in a seeded air plasma. Measured conductivities for the nitrogen plasma were on the order of 2 to 3 times larger than comparable measurements for the air plasma, whereas the CEC with the Demetriades–Argyropoulas conductivity model produced comparable results for the two plasmas. The experiments indicated that there are practical problems in ensuring a good seed distribution within the test gas. This problem will be just as important in a continuous-flow environment. It must therefore be addressed before a test facility employing an MHD accelerator can be feasible.
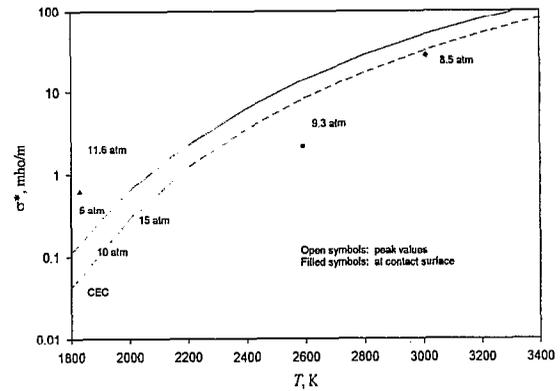
References

[1] Nelson, G.L. and Simmons, G.A., "Report on the NASA Mariah Project and Summary of Technical Results," AIAA Paper 98–2752, 1998.

[2] Nelson, G.L. and Simmons, G.A., "Augmentation of Hypersonic Propulsion Test Facilities Using MHD," AIAA Paper 95–1937, 1995.

[3] Litchford, R., Thompson, B., Lineberry, J. and Lin, B., "Pulse Detonation MHD Experiments," AIAA Paper 98–2918, 1998.

[4] Cambier, J.-L., "MHD Power Extraction from a Pulse Detonation Engine," AIAA Paper 98–3876, 1998.

[5] Lu, F.K., Kim, C.H., Wilson, D.R., Liu, H.-C., Stuessy, W.S. and Simmons, G.A., "Exploratory Study of Gas Conductivity in Detonation Waves," AIAA Paper 99–0868, 1999.

[6] Brichkin, D.I., Kuranov, A.L. and Sheikin, E.G., "MHD-Technology for Scramjet Control," AIAA Paper 98–1642, 1998.

[7] Chinitz, W., Erdos, J.I., Rizkalla, O., Anderson, G.Y. and Bushnell, D.M., "Facility Opportunities and Associated Stream Chemistry Considerations for Hypersonic Air-Breathing Propulsion," AIAA Journal of Propulsion and Power, Vol. 10, No. 1, 1994, pp. 6–17.

[8] Garrison, G. W., "Electrical Conductivity of a Seeded Nitrogen Plasma," AIAA Journal, Vol. 6, No. 7, 1968, pp. 1264–1270.

[9] Pate, S.R., Siler, L.G., Stallings, D.W. and Wagner, D.A., "Development of an MHD-Augmented, High Enthalpy, Shock Tunnel Facility," AIAA Journal, Vol. 12, No. 3, 1974, pp. 289–297.

[10] Stuessy, W.S., Lu, F.K. and Wilson, D.R., "Shock-Induced Detonation Wave Driver for Enhancing Shock Tube Performance," AIAA Paper 98–0549, 1998.

[11] Alpher, R.A. and White, D.R., "Flow in Shock Tubes with Area Change at the Diaphragm Section," Journal of Fluid Mechanics, Vol. 3, 1958, pp. 457–470.

[12]Liu, H.-C., Stuessy, W.S., Lu, F.K. and Wilson, D.R., "Design of an Electrical Conductivity Channel for Shock Tunnel," AIAA Paper 96–2198, 1996.

[13]Lin, S.C., Resler, E.L. and Kantrowitz, A., "Electrical Conductivity of Highly Ionized Argon Produced by Shock Waves, *Journal of Applied Physics*, Vol. 26, No. 1, 1953, p. 95.

[14]Spitzer, L. and Harm, R., "Transport Phenomena in a Completely Ionized Gas," *The Physical Review*, Vol. 89, 1963, p. 977.

[15]Vincenti, W.G. and Kruger, C.H., *Introduction to Physical Gas Dynamics*, Krieger, Huntington, New York, 1977.

[16]Gordon, S. and McBride, B.J., "Computer Program for Calculation of Complex Chemical Equilibrium Compositions, Rocket Performance, Incident and Reflected Shocks, and Chapman-Jouguet Detonations," NASA SP-273, 1976.

[17]Demetriades, S.T and Argyropoulas, G.S., "Ohm's Law in Multicomponent Nonisothermal Plasmas with Temperature and Pressure Gradients," *Physics of Fluids*, Vol. 8, No. 11, 1966, pp. 2136–2149.

[18]Wilson, D.R., Lu, F.K., Stuessy, W.S. and Burge, K.R., "Development of a High-Pressure Detonation-Driven Shock Tube Facility," AIAA Paper 96–0853, 1996.

[19]Lu, F.K., Wilson, D.R., Stuessy, W.S., Bakos, R.J. and Erdos, J.I., "Recent Advances in Detonation Techniques for High-Enthalpy Facilities," AIAA Paper 98–0550, 1998.

[20]Adler, R.J., *Pulse Power Formulary*, North Star Research Corporation, Albuquerque, New Mexico, 1989.

[21]Simmons, G.A., private communication, July 31, 1997.

[22]Nottingham, W.B., "A New Equation for the Static Characteristic of the Normal Electric Arc," *Transactions of the AIEE*, 1923, pp. 302–310.

[23]Liu, H.-C., "Electrical Conductivity Measurement of a High-Pressure Seeded Air Plasma," Ph.D. Dissertation, University of Texas at Arlington, 1998.

[24]Simmons, G.A., Nelson, G.L. and Ossello, C.A., "Electron Attachment in Seeded Air for Hypervelocity MHD Accelerator Propulsion Wind Tunnel Applications," AIAA Paper 98–3133, 1998.